Microsc. Microanal. 19, S5, 114–118, 2013
doi:10.1017/S1431927613012452

Enhanced Morphological and Thermal Stabilities of Nickel Germanide with an Ultrathin Tantalum Layer Studied by *Ex Situ* and *In Situ* Transmission Electron Microscopy

Jae-Wook Lee,[1] Hyung-Kyu Kim,[1] Jee-Hwan Bae,[1] Min-Ho Park,[1] Hyoungsub Kim,[1] Jiho Ryu,[2] and Cheol-Woong Yang[1,*]

[1]*School of Advanced Materials Science & Engineering, Sungkyunkwan University, Suwon 440-746, South Korea*
[2]*Department of Automobile Development, Ajou Motor College, Boryeong 355-769, South Korea*

Abstract: The formation and morphological evolution of germanides formed in a ternary Ni/Ta-interlayer/Ge system were examined by *ex situ* and *in situ* annealing experiments. The Ni germanide film formed in the Ni/Ta-interlayer/Ge system maintained continuity up to 550°C, whereas agglomeration of the Ni germanide occurred in the Ni/Ge system without Ta-interlayer. Through microstructural and chemical analysis of the Ni/Ta-interlayer/Ge system during and after *in situ* annealing in a transmission electron microscope, it was confirmed that the Ta atoms remained uniformly on the top of the newly formed Ni germanide layer during the diffusion reaction. Consequently, the agglomeration of the Ni germanide film was retarded and the thermal stability was improved by the Ta incorporation.

Key words: Ni germanide, thermal stability, *in situ* TEM, Ta-interlayer, agglomeration, AEM

Introduction

Because of the ever-increasing demand for scaling down metal-oxide-semiconductor field-effect transistor (MOSFET) devices, Si-based devices are approaching their fundamental limit. Recently, Ge has been considered as an attractive replacement for Si substrate in high-performance transistors because of its higher carrier mobility. Compared with Si, Ge offers two times higher intrinsic electron mobility and four times higher intrinsic hole mobility (Martin et al., 1989; Lee et al., 2001; Shang et al., 2003; Saraswat et al., 2006), and these enhanced mobilities result in larger saturated drain currents, enhanced transconductance, and higher cutoff frequencies (Spann et al., 2005). However, there are several problems in realizing Ge-based MOSFETs, such as the inferior thermal stability and water solubility of Ge oxides. Successful studies on Ge MOSFETs with high-*k* gate dielectric such as Ge oxynitride, HfO_2, and ZrO_2 have been demonstrated recently (Gusev et al., 2004; Bai et al., 2006; Oh et al., 2007). These very promising results suggest that the use of Ge channels will allow MOSFET technology to be extended beyond the limitations imposed by the material properties of Si.

In order to fully exploit the superior transport properties of Ge, a low-resistance contact technology will have to be developed based on metal germanides. A self-aligned germanide through the solid-phase reactions of Ge and metals, such as Ti, Co, and Ni, in much the same way as self-aligned silicide, is known to be effective in reducing the parasitic source/drain resistance (Ashburn et al., 1992; Patterson et al., 1994; Park et al., 2009). Of these metal germanides, the Ni germanide is highly attractive as a promising self-aligned germanide material for Ge MOSFET technology because of its low processing temperature and low resistivity (Hsu et al., 2005; Zhang et al., 2005). However, the poor thermal stability of Ni germanide due to agglomeration is one major drawback. Several methods to slightly improve the thermal stability of Ni germanide such as using Ni alloy targets and ultrathin Ti and Yb interlayers have been reported (Liew et al., 2006; Zhu et al., 2007; Zhang et al., 2009).

This study examined the formation and microstructural evolution of Ni germanide utilizing an ultrathin Ta interlayer as a function of annealing temperature using *ex situ* and *in situ* annealing experiments. The *in situ* annealing experiments were carried out in a transmission electron microscope (TEM) equipped with a specimen heater. And various analytical electron microscopy (AEM) techniques were used to investigate the microstructure and chemical composition of the phase formed by the reaction.

Materials and Methods

First, *p*-type (1 0 0) Ge substrates were RCA cleaned and dipped cyclically into a dilute hydrofluoric acid (HF) solution ($HF:H_2O = 1:100$) and deionized water for 30 s, respectively, five times, and were immediately loaded into a DC magnetron sputtering system. Then ~2-nm-thick Ta and 13-nm-thick Ni films were deposited sequentially at room temperature in a 5.0 mtorr using Ar gas after reaching a base pressure below 2.0×10^{-7} torr. A cross-sectional high-resolution (HR) TEM micrograph of the as-deposited specimen of the Ni/Ta-interlayer/Ge system formed by this way was shown in the inset of Figure 1. Approximately 15-nm-thick Ni film alone was also deposited on Ge substrates for comparison. For the formation of Ni germanide, *ex situ* and

*Corresponding author. E-mail: cwyang@skku.edu

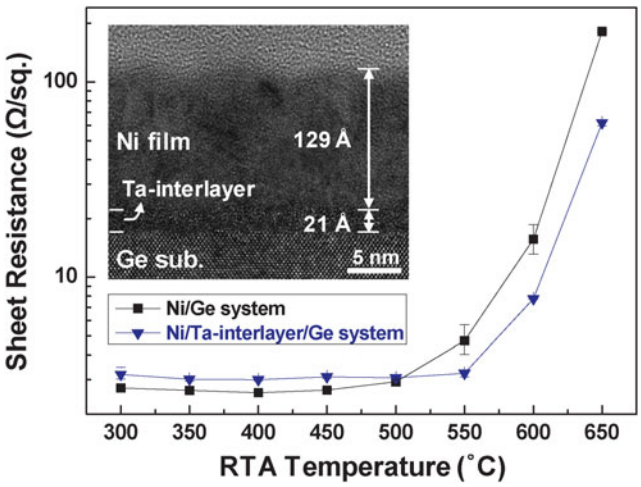

Figure 1. The R_s values of the Ni/Ge and Ni/Ta-interlayer/Ge systems after rapid thermal annealing (RTA) in the temperature range between 300 and 650°C for 60 s in N_2 ambient. Inset shows a cross-sectional high-resolution transmission electron microscope micrograph of the as-deposited specimen of the Ni/Ta-interlayer/Ge system formed by this experimental procedure.

in situ annealing experiments were carried out. For the *ex situ* annealing experiment, each sample was annealed by rapid thermal annealing (RTA) at every 50°C temperature interval in the temperature range from 300 to 650°C for 60 s in N_2 ambient. The unreacted metal layer was selectively removed from a diluted phosphoric acid (H_3PO_4) solution. The sheet resistance (R_s) was measured by using a four-point probe system. The microstructures and chemical compositions of the specimens were characterized by AEM (JEM-2100F, JEOL Co. Ltd.) equipped with scanning transmission electron microscope (STEM)/energy-dispersive spectrometer (EDS). TEM specimens were prepared using a tripod polisher for mechanical grinding and Ar-ion milling, and the TEM specimens for the *in situ* annealing experiment were fixed on Mo oval grids in order to reduce the occurrence of thermal drift phenomena due to thermal expansion. The *in situ* annealing experiment was carried out in a TEM (JEM-3011, JEOL Co. Ltd.) with a specimen heating-tilting holder (EM-31050, JEOL Co. Ltd.) and a heater control unit (EM-SHU2, JEOL Co. Ltd.). The images were recorded by using a CCD camera (2k Gatan Ultrascan) and a digital video recording system with a 1/30 s time resolution (30 frames/s) connected to a TV rate camera.

Results and Discussion

In order to compare the thermal stability of Ni germanides formed from the Ni/Ge and Ni/Ta-interlayer/Ge systems, the specimen were annealed by RTA at the temperature range between 300 and 650°C for 60 s. Figure 1 shows the R_s values of the specimens with and without the Ta-interlayer as a function of annealing temperature. For all the specimens of both systems, the measured R_s values were almost constant (~3 Ω/sq.) up to 500°C, above which the measured R_s values in the Ni/Ge system increased abruptly. It is

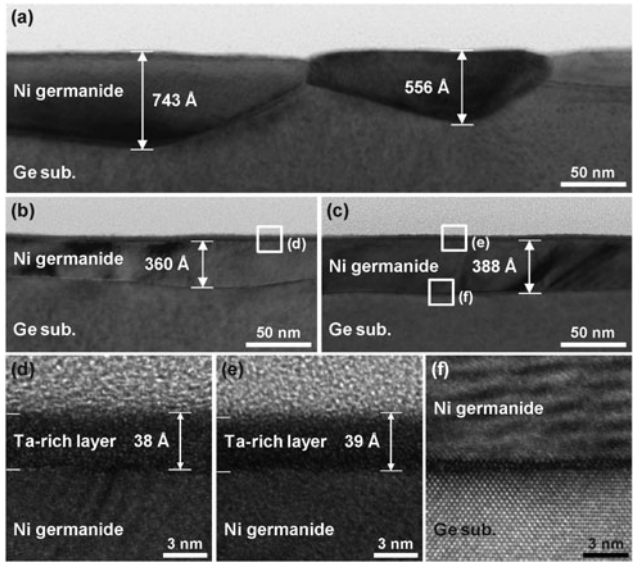

Figure 2. Cross-sectional transmission electron microscope (TEM) micrographs: (**a**) the Ni/Ge system annealed by rapid thermal annealing (RTA) at 550°C for 60 s in N_2 ambient, and the Ni/Ta-interlayer/Ge system annealed by RTA at (**b**) 300°C and (**c**) 550°C, and high-resolution TEM micrographs of two interfaces: Ta-rich layer/Ni germanide in specimens annealed at (**d**) 300°C and (**e**) 550°C, and (**f**) Ni germanide/Ge substrate.

noteworthy that the measured R_s value of the specimen annealed at 550°C in the Ni/Ta-interlayer/Ge system maintained almost constant value which was measured by specimens annealed at lower temperatures. In the case of Ni germanide, the degradation of the R_s value by high-temperature annealing can be explained in terms of the agglomeration of NiGe (Park et al., 2007). For the Ni/Ta-interlayer/Ge system, the thermal stability of Ni germanide was improved, probably because of the retardation of the agglomeration process by the Ta atoms, which are discussed in detail in the following paragraphs.

Figure 2a shows a cross-sectional TEM micrograph of the Ni/Ge system annealed by RTA at 550°C, where the R_s value doubly increased the initial values. The Ni germanide grains grew to ~55–75 nm in thickness, and became irregular with thermal grooves between the germanide grains on the surface and at the interface between the germanide and the Ge substrate. In addition, separations of the germanide layer due to agglomeration of germanide grains were observed in several places (not shown). In the case of the Ni/Ta-interlayer/Ge system, an ~35-nm-thick continuous and uniform Ni germanide layer was observed on the Ge substrate in the specimen annealed at 300°C (see Fig. 2b). And the growth of Ni germanide grains was suppressed and a continuous and uniformly thick Ni germanide layer (<40-nm-thick) was observed in the specimen annealed at 550°C (see Fig. 2c). It is notable that the existence of the dark layer was observed on top of the germanide layer in the Ni/Ta-interlayer/Ge system. Figures 2d–2f show the enlarged HR-TEM images of the two interfaces, i.e., the ambient/NiGe and the NiGe/Ge substrate, which were indicated by white

https://doi.org/10.1017/S1431927613012452 Published online by Cambridge University Press

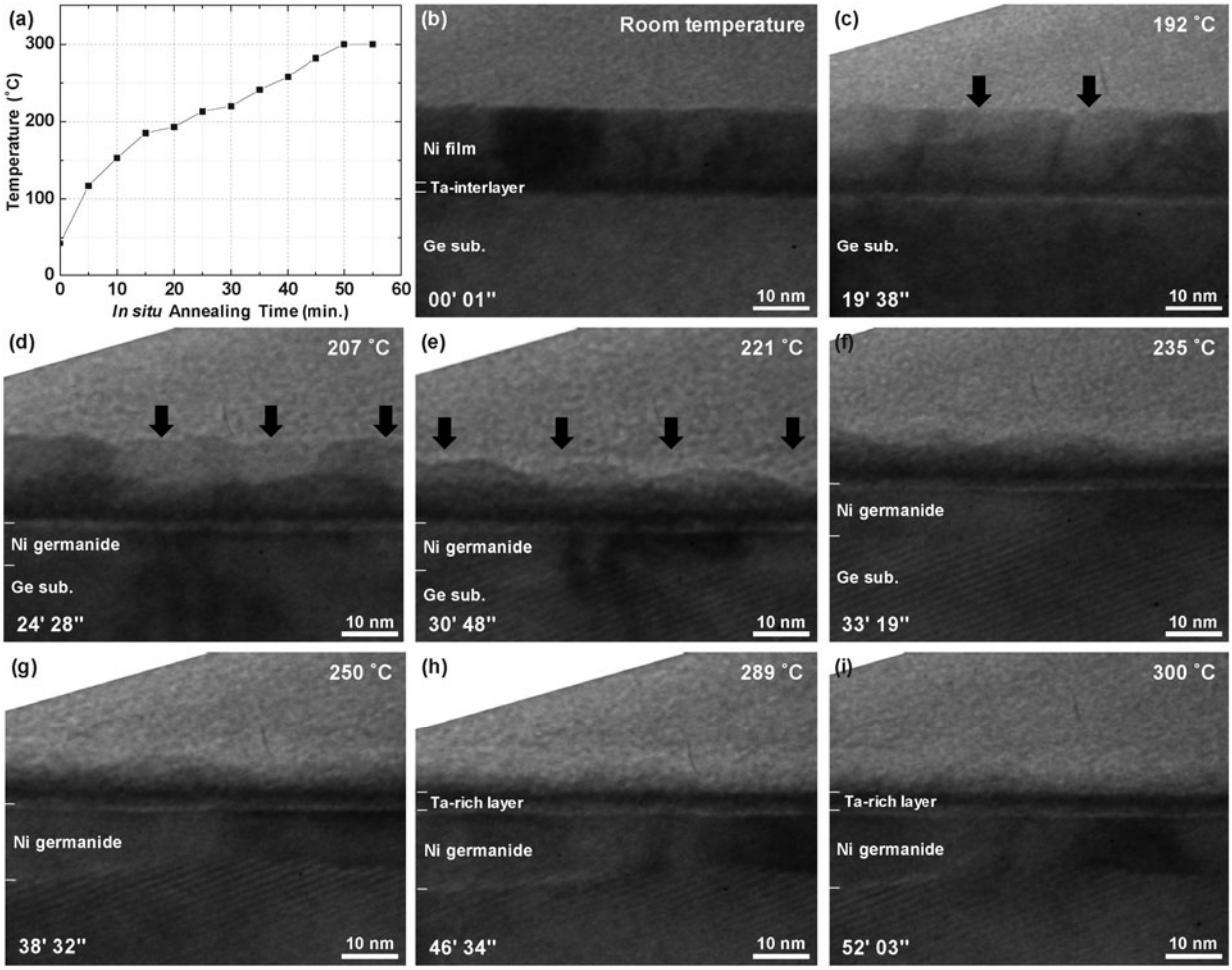

Figure 3. a: The temperature profile of the *in situ* annealing experiment. **b–i:** Individual frames selected from video sequence recorded during the *in situ* annealing of a cross-section of the Ni/Ta-interlayer/Ge system at temperature ranging from room temperature to 300°C.

squares in Figures 2b and 2c. Approximately 4-nm-thick amorphous layers were formed on the NiGe films, as shown in Figures 2d and 2e. These additional layers were confirmed to be a Ta-rich layer by EDS analysis. The compositions of the Ta-rich layers of the specimens annealed at 300 and 550°C were similar to each other and 44.60 ± 1.26 at.% Ta, 21.56 ± 2.13 at.% Ni, 33.84 ± 2.62 at.% Ge, and 44.35 ± 1.30 at.% Ta, 21.37 ± 2.23 at.% Ni, 34.28 ± 2.72 at.% Ge, respectively. And the interface between NiGe and the Ge substrate was clean, without any interfacial layer (see Fig. 2f). The agglomeration, which is a major cause of the increased R_s value of Ni germanide, is derived from the driving force of the decreased interfacial energy or surface energy. It is believed that the Ta-rich layer acts to reduce the surface free energy of NiGe film with outside ambient. Thus, the agglomeration is retarded because of the formation of the Ta-rich layer on the top of the Ni germanide layer.

In order to obtain a better understanding of the formation and microstructural evolution of the germanide and Ta-rich top layer in the Ni/Ta-interlayer/Ge system, a direct observation of the reactions were carried out using *in situ* annealing TEM. Figure 3a shows the temperature profile of the *in situ* annealing experiment, and the heating rate was ~5.16°C/min. Figures 3b–3i show a series of individual frames selected from a video sequence recorded during the *in situ* annealing of a cross-section of the Ni/Ta-interlayer/Ge system at temperature ranging from room temperature to 300°C. The as-deposited specimen of Ni/Ta-interlayer/Ge system at room temperature was revealed in Figure 3b, and this is essentially the same as the specimen used for *ex situ* annealing experiments. As the annealing temperature was increased to 193°C (see Fig. 3c), the upper parts of the Ni film indicated by the arrows began to vacate. When the annealing temperature was increased to 207°C, the vacated parts near the surface of the film indicated by the arrows became larger (see Fig. 3d), and Ni germanide grains began to form by diffusion of the Ni atoms into Ge substrate through the Ta-interlayer. As the annealing temperature increased, the remaining film thickness decreased gradually and the Ni germanide grain grew thicker, as shown in Figures 3e–3h. When the annealing temperature was increased up to 300°C, an ~15-nm-thick Ni germanide layer was formed and an ~3-nm-thick film remained on top of the newly formed Ni germanide layer (see Fig. 3i).

https://doi.org/10.1017/S1431927613012452 Published online by Cambridge University Press

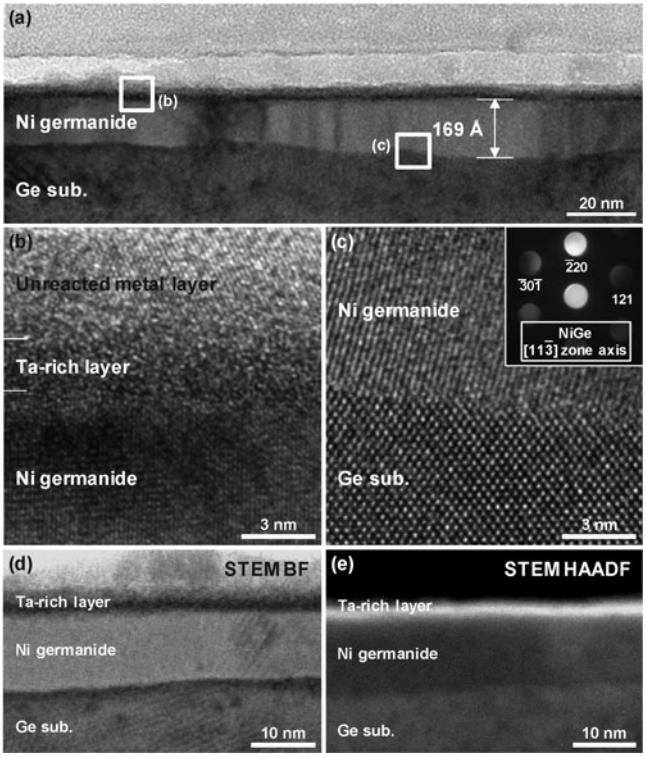

Figure 4. a: Low-magnification transmission electron microscope (TEM) micrograph of the *in situ* annealed specimen after annealing up to 300°C, and high-resolution TEM micrographs of two interfaces. **b:** Ta-rich layer/Ni germanide and (**c**) Ni germanide/Ge substrate and nano-beam electron diffraction pattern obtained from a Ni germanide grain (inset), and scanning transmission electron microscope (**d**) bright field and (**e**) high-angle annular dark-field micrographs of the *in situ* annealed specimen.

For the characterization of the phases formed during the *in situ* annealing experiment, the microstructure and chemical composition were examined by using AEM equipped with STEM/EDS. Figure 4 shows the TEM micrographs of the specimen annealed for up to 300°C along with nano-beam electron diffraction (NBED) pattern obtained from the Ni germanide grain. The surface morphology of the Ta-rich layer and Ni germanide was relatively uniform; however, the interface between the Ni germanide and Ge substrate was slightly rougher than one of the *ex situ* annealed specimens (see Fig. 4a). Nevertheless, as shown in the HR-TEM micrographs of Figures 4b and 4c, the Ta-rich layer and the phase of Ni germanide formed from *in situ* annealing process were similar to one of *ex situ* annealed specimens. The average composition of the Ta-rich layer was 44.45 ± 1.73 at.% Ta, 21.16 ± 2.97 at.% Ni, and 34.38 ± 3.60 at.% Ge as measured by STEM/EDS utilizing a 0.7 nm electron probe. As shown in the STEM bright field (see Fig. 4d) and high-angle annular dark-field (HAADF, see Fig. 4e) micrographs, the contrast of the Ta-rich layer was distinct from the other phases. Considering the contrast mechanisms of STEM imaging, this difference in contrast was attributed to a mass-thickness effect on STEM imaging. Ta is the heaviest element among the components and is brighter in the STEM/HAADF image. And the NBED pattern (see the inset of Fig. 4c) obtained from a Ni germanide grain was indexed as the $[11\bar{3}]$ zone axis pattern of NiGe, which has an orthorhombic structure: a = 5.811, b = 5.381, and c = 3.428 Å. This is consistent with the STEM/EDS result of 50.35 ± 2.01 at.% Ni and 49.65 ± 1.63 at.% Ge, which is close to the stoichiometric NiGe composition. Therefore, the phase of Ni germanide formed using this *in situ* annealing experiment was confirmed to be a Ni mono-germanide (NiGe). No other form of germanide was observed in this study.

The formation process of the Ni germanide and the Ta-rich layer in the Ni/Ta-interlayer/Ge system was analogous to one in the Ni–Ta alloy/Ge system of our previous work (Lee et al., 2008). Several intermetallic compounds can be present in the Ta–Ge system. However, they cannot be formed under this annealing condition. In addition, the solid solubility of Ta in Ge is extremely low even at high temperature. Consequently, most of Ta atoms cannot diffuse into the Ge substrate and remain on top of the newly formed NiGe film. The presence of a Ta-rich layer on top of the Ni germanide layer likely modified the interfacial energies and suppressed the agglomeration of NiGe grains, thus improving the surface morphology of the Ni germanide formed in the Ni/Ta-interlayer/Ge system. As a result, the thermal stability of the Ni/Ta-interlayer/Ge system was better than that of the Ni/Ge system.

Conclusions

This study examined the formation and morphological evolution of germanides formed in Ni/Ge and Ni/Ta-interlayer/Ge systems as a function of the annealing temperature using *ex situ* and *in situ* annealing experiments. The Ni/Ta-interlayer/Ge system improved the thermal stability and maintained low R_s value up to 550°C. For the Ni/Ge system annealed by RTA, severe agglomeration began to occur at an annealing temperature of 550°C. On the other hand, in the case of the Ni/Ta-interlayer/Ge system, less agglomeration and a uniform surface morphology were observed under the same annealing condition. It is confirmed that the Ta-rich layer formed because Ta atoms remained on top of the newly formed Ni germanide film through AEM analysis of the Ni/Ta-interlayer/Ge system during and after the *in situ* annealing experiments. Eventually, the surface free energy of the Ni germanide film was reduced by this Ta-rich layer, and the thermal stability of the Ni germanide was improved.

Acknowledgments

This work was supported by the National Research Foundation of Korea (NRF) grants funded by the Korea government (MEST, No. 2011-0017257, No. 2011-0019984, and No. 2011-0030803). The authors gratefully appreciate technical support from the cooperative center for research facilities (CCRF) at Sungkyunkwan University.

References

Ashburn, S.P., Öztürk, M.C., Wortman, J.J., Harris, G., Honeycutt, J. & Maher, D.M. (1992). Formation of titanium and cobalt germanides on Si (100) using rapid thermal processing. *J Electron Mater* **21**, 81–86.

Bai, W.P., Lu, N., Ritenour, A., Lee, M.L., Antoniadis, D.A. & Kwong, D.L. (2006). Ge n-MOSFETs on lightly doped substrates with high-*k* dielectric and TaN gate. *IEEE Electron Device Lett* **27**, 175–178.

Gusev, E.P., Shang, H., Copel, M., Gribelyuk, M., D'emic, C., Kozlowski, P. & Zabel, T. (2004). Microstructure and thermal stability of HfO_2 gate dielectric deposited on Ge(100). *Appl Phys Lett* **85**, 2334–2336.

Hsu, S.L., Chien, C.H., Yang, M.J., Huang, R.H., Leu, C.C., Shen, S.W. & Yang, T.H. (2005). Study of thermal stability of nickel monogermanide on single- and polycrystalline germanium substrates. *Appl Phys Lett* **86**, 251906.

Lee, J.W., Bae, J.H., Park, M.H., Kang, H.B., Kim, H. & Yang, C.W. (2008). Microstructural evolution of nickel-germanide in the $Ni_{1-x}Ta_x$/Ge systems during *in situ* annealing. *J Vac Sci Technol A* **26**, 688–691.

Lee, M.L., Leitz, C.W., Cheng, Z., Pitera, A.J., Currie, M.T., Taraschi, G., Fitzgerald, E.A. & Antoniadis, D.A. (2001). Strained Ge channel *p*-type metal-oxide-semiconductor field-effect transistors grown on $Si_{1-x}Ge_x$/Si virtual substrates. *Appl Phys Lett* **79**, 3344–3346.

Liew, S.L., Lee, R.T.P., Lee, K.Y., Balakrisnan, B., Chow, S.Y., Lai, M.Y. & Chi, D.Z. (2006). Enhanced morphological stability of NiGe films formed using Ni(Zr) alloy. *Thin Solid Films* **504**, 104–107.

Martin, S.C., Hitt, L.M. & Rosenberg, J.J. (1989). P-channel germanium MOSFET's with high channel mobility. *IEEE Electron Device Lett* **10**, 325–326.

Oh, J., Majhi, P., Kang, C.Y., Yang, J.W., Tseng, H.H. & Jammy, R. (2007). Thermal stability of nanoscale Ge metal-oxide-semiconductor capacitors with ZrO_2 high-*k* gate dielectrics on Ge epitaxial layers. *Appl Phys Lett* **90**, 202102.

Park, K., An, C.H., Lee, M.S., Yang, C.W., Lee, H.J. & Kim, H. (2009). Microstructural evolution and electrical characteristics of Co-germanide contacts on Ge. *J Electrochem Soc* **156**, H229–H232.

Park, K., Lee, B.H., Lee, D., Ko, D.H., Kwak, K.H., Yang, C.W. & Kim, H. (2007). A study on the thermal stabilities of the NiGe and $Ni_{1-x}Ta_xGe$ systems. *J Electrochem Soc* **154**, H557–H560.

Patterson, J.K., Park, B.J., Ritley, K., Xiao, H.Z., Allen, L.H. & Rockett, A. (1994). Kinetics of Ni/a-Ge bilayer reactions. *Thin Solid Films* **253**, 456–461.

Saraswat, K., Chui, C.O., Krishnamohan, T., Kim, D., Nayfeh, A. & Pethe, A. (2006). High performance germanium MOSFETs. *Mat Sci Eng B* **135**, 242–249.

Shang, H., Okorn-Schimdt, H., Ott, J., Kozlowski, P., Steen, S., Jones, E.C., Wong, H.S.P. & Hanesch, W. (2003). Electrical characterization of germanium p-channel MOSFETs. *IEEE Electron Device Lett* **24**, 242–244.

Spann, J.Y., Anderson, R.A., Thornton, T.J., Harris, G., Thomas, S.G. & Tracy, C. (2005). Characterization of nickel germanide thin films for use as contacts to p-channel germanium MOSFETs. *IEEE Electron Device Lett* **26**, 151–153.

Zhang, Q., Wu, N., Osipowicz, T., Bera, L.K. & Zhu, C. (2005). Formation and thermal stability of nickel germanide on germanium substrate. *Jpn J Appl Phys* **44**, L1389–L1391.

Zhang, Y.Y., Oh, J., Li, S.G., Jung, S.Y., Park, K.Y., Shin, H.S., Lee, G.W., Wang, J.S., Majhi, P., Tseng, H.H., Jammy, R., Bae, T.S. & Lee, H.D. (2009). Ni germanide utilizing ytterbium interlayer for high-performance Ge MOSFETs. *Electrochem Solid-State Lett* **12**, H18–H20.

Zhu, S., Yu, M.B., Lo, G.Q. & Kwong, D.L. (2007). Enhanced thermal stability of nickel germanide on thin epitaxial germanium by adding an ultrathin titanium layer. *Appl Phys Lett* **91**, 051905.